Thermal Degradation Kinetics of Completely Biodegradable and Biobased PLA/PHB Blends

Magdalena L. Iglesias-Montes , David A. D'Amico , Luciana B. Malbos , Irene T. Seoane , Viviana P. Cyras , Liliana B. Manfredi

PII: S0040-6031(23)00099-0
DOI: https://doi.org/10.1016/j.tca.2023.179530
Reference: TCA 179530

To appear in: *Thermochimica Acta*

Received date: 28 January 2023
Revised date: 8 May 2023
Accepted date: 9 May 2023

Please cite this article as: Magdalena L. Iglesias-Montes , David A. D'Amico , Luciana B. Malbos , Irene T. Seoane , Viviana P. Cyras , Liliana B. Manfredi , Thermal Degradation Kinetics of Completely Biodegradable and Biobased PLA/PHB Blends, *Thermochimica Acta* (2023), doi: https://doi.org/10.1016/j.tca.2023.179530

Highlights

- Thermal degradation kinetics of biodegradable polymer blends was evaluated
- Kissinger-Akahira-Sunose and Vyazovkin isoconversional methods were applied
- The composition and morphology of the blends influenced their thermal behavior
- The addition of nanochitin diminished the effective activation energy of the blends
- Avrami-Erofeev function was the most probable kinetic mechanism of the systems studied

Thermal Degradation Kinetics of Completely Biodegradable and Biobased PLA/PHB Blends

Magdalena L. Iglesias-Montes[1], David A. D'Amico[1], Luciana B. Malbos[1], Irene T. Seoane[1], Viviana P. Cyras[1], Liliana B. Manfredi[1,*]

[1] Instituto de Investigaciones en Ciencia y Tecnología de Materiales (INTEMA), Facultad de Ingeniería, Universidad Nacional de Mar del Plata—Consejo de Investigaciones Científicas y Técnicas (CONICET), 7600 Mar del Plata, Argentina; mliglesias@fi.mdp.edu.ar (MLIM); dadamico@fi.mdp.edu.ar (DAD); lucianamalbos@fi.mdp.edu.ar (LM); itseoane@fi.mdp.edu.ar (ITS); vpcyras@fi.mdp.edu.ar (VPC)

*Correspondence to: lbmanfre@fi.mdp.edu.ar (LBM); tel.: +54-2236260600

Abstract

In this article, the influence of blend ratio of plasticized poly(lactic acid)/poly(3-hydroxybutyrate) (PLA/PHB) and chitin nanoparticles (ChNP) nanocomposites on the thermal stability and degradation kinetics has been investigated using thermogravimetric analysis under nitrogen atmosphere at four different heating rates (i.e., 5, 15, 30, and 50 °C/min). The derivative thermogravimetric curves have indicated single-step and two-step degradation processes for individual polymers and polymer blends, respectively. It suggests immiscibility or partial miscibility between the polymers. The degradation kinetic parameters were studied over the 30 – 500 °C temperature range by using the Kissinger-Akahira-Sunose (KAS) and Vyazovkin isoconversional methods under non-isothermal conditions. The average values of the effective activation energies of the deconvoluted PHB and PLA peaks in the PLA:PHB 70:30 (B73) blends were higher than those of the pure polymers, while in the PLA:PHB 60:40 (B64) blends were lower, which was attributed to the different morphology of the blends. Furthermore, the effective activation energy of the nanocomposites diminished due to the catalyzing effect of the chitin nanoparticles. By means of the invariant kinetic parameters (IKP) method, it was possible to evaluate the preexponential factor and the activation energy of the blends without any assumptions concerning kinetic model. The invariant activation energies calculated were in accordance with the ones estimated by the isoconversional methods. Finally, Avrami-Erofeev function was determined as the most probable kinetic mechanism of the systems studied by applying the Sestak-Berggren equation.

Keywords Poly(lactic acid); Poly(3-hydroxybutyrate); Bio-based; Biodegradable polymers; Kinetic analysis; Thermal degradation

1. Introduction

There is an urgent need for the development of green polymeric materials that would not involve the use of toxic components in their manufacture and that could be degraded into natural environmental products. For these reasons, throughout the world today, the development of biodegradable materials with controlled properties has been a subject of great research challenge to the community of material scientists and engineers [1]. Preparation of blends is among the routes to improve some properties of biodegradable polymers such as thermal oxidative stability, mechanical properties, moisture absorption, etc.

Polyhydroxyalkanoates (PHAs) represent an interesting alternative to synthetic polymers due to many advantages. They are not only biodegradable and biocompatible, but they can also be produced by bacterial fermentation from renewable resources like sugar cane. Poly(3-hydroxybutyrate) (PHB), the most commonly used PHA, was first discovered in 1926 by Lemoigne [2]. Nevertheless, there are many factors which limit its use on industrial scale such as high stiffness, brittleness and poor thermal stability at temperatures just above the melting point [3].

Poly(lactic acid) (PLA) is a semi-crystalline thermoplastic polyester derived from lactic acid monomer, which, in turn, is obtained from the fermentation of renewable resources rich in carbohydrates like corn starch, sugar beet and wheat [4]. PLA is also biocompatible, compostable and it is immunologically inactive and non-toxic. It presents high transparency and has greater mechanical strength and easier processability than PHB. Although PLA is compatible with many current processing techniques, the fact that it has a high glass transition temperature (50 – 80 °C) leads to brittleness in the final products [5].

Several authors have studied blends of PLA/PHB in the last decades [6–12] to improve properties of both PLA and PHB. In general, it was reported that PLA/PHB mixtures exhibit better barrier properties than pure PLA due to the presence of semi-crystalline PHB. Plasticized blends have also been formulated by using tributyrin (TB) [13,14], limonene [15] and polyethylene glycol (PEG) [16], among others.

Nanoscience has as well been put into practice for the preparation of polymer blends in order to get better physical, chemical and functional properties [17]. In fact, the application of nanotechnology techniques could improve physical properties of biopolymers, including mechanical strength, thermal stability, and barrier properties against the permeability of oxygen, carbon dioxide, flavor compounds, and water vapor. Chitin nanoparticles (ChNP) are a nano-reinforcement that has drawn a lot of attention in the field of green nanotechnology in recent years, and have also been used to develop PLA/PHB nanocomposites [18,19]. In our previous work [19] it was found that the addition of PHB and ChNPs influenced the crystallinity of the plasticized PLA, enhancing its barrier and optical properties. Moreover, the ChNPs improved the overall migration behavior of blends.

Much information is available on investigations of PLA/PHB blends; however, parameters such as thermal degradation kinetics have not been extensively studied yet. In many industrial processes, there are a number of operational variables that must be controlled in order to avoid the degradation of the raw materials. In order to know the materials' processing temperature limits, it is necessary to characterize their thermal degradation behavior. In this sense, studying the kinetics of polymers' thermal degradation is crucial to understand this process in detail [20].

The thermal stability of polymeric materials is usually studied by thermogravimetric (TGA) analysis. The weight loss due to the formation of volatile products during degradation at high temperature is monitored as a function of temperature. The aim of the kinetic analysis is the determination of kinetic triplet (i.e. kinetic model, $f(\alpha)$, activation energy, E, and pre-exponential factor, A) for the investigated process. By its nature the macroscopic kinetics are complex as they include information about simultaneously occurring multiple steps. Unraveling macroscopic kinetics presents a challenge that can only be overcome by computational methods that allow the detection and treatment of multi-step processes. Isoconversional and multi-heating rate methods are among a few methods that are up to this challenge [21]. These methods require performing a series of experiments at different temperature programs and yield the dependence of the activation energy (E) on conversion (α). This dependence can be used to explore the mechanisms of processes and to predict kinetics [22].

The present investigation is focused on the analysis of the thermal degradation kinetics of biodegradable polymer blends based on PLA and PHB, plasticized with tributyrin and reinforced with chitin nanoparticles, complementing the characterization of the materials formulated on our previous works [14,19,23]. The PLA:PHB weight ratios used for blends were 70:30 and 60:40, while the proportion of TB and ChNP incorporated were 15 wt% and 2 wt%, respectively, of the final weight sample [14,19,23]. As far as we know, there is no bibliography concerning the kinetic analysis of the non-isothermal degradation of PLA/PHB/TB/ChNP nanocomposites. In this context, the aim of this work was to study the effect of the blend composition on the thermal stability and thermal degradation kinetics by using TGA. Four different heating rates were chosen for the analysis. Isoconversional Kissinger-Akahira-Sunose (KAS) [24] and Vyazovkin [22]

methods in combination with the invariant kinetic parameters (IKP) [25] method were used to calculate the kinetic triplet of all the materials.

2. Theoretical backgrounds of thermal degradation kinetics

According to kinetic theory, thermal decomposition of a solid-state sample can be expressed as a single-step reaction by using **Eq. (1)**:

$$\frac{d\alpha}{dt} = k(T)f(\alpha) \quad \textbf{(1)}$$

where *t* is the time, *k(T)* is the rate constant, *T* is the temperature, *f(α)* is the reaction model that represents the degradation mechanism and *α* is the conversion or extent of reaction, which can be determined from TGA runs as a fractional mass loss as described below:

$$\alpha = \frac{m_0 - m(T)}{m_0 - m_f} \quad \textbf{(2)}$$

where m_0 and m_f denote the initial and residual mass, respectively, and *m(T)* refers to the actual mass of the sample at a selected temperature.

In general, the temperature dependence of the rate constant, *k(T)*, is expressed by the Arrhenius equation, as follows:

$$k(T) = A.exp\left(\frac{-E}{RT}\right) \quad \textbf{(3)}$$

where *A* is a pre-exponential factor, *E* is the activation energy and *R* is the gas constant. The kinetic parameters that are experimentally determined, are appropriate to be called "apparent" or "effective" to emphasize the fact that they may deviate from the intrinsic parameters of a given individual step process. That is why, from here on, the term "apparent/effective activation energy" will be used frequently.

For non-isothermal data, usually the temperature varies linearly with time, then the heating rate (β) can be written as:

$$\beta = \frac{dT}{dt} = const \quad \textbf{(4)}$$

Combining the Eqs. **(1)**, **(3)** and **(4)**, the following expression is obtained:

$$\beta \frac{d\alpha}{dT} = A.exp\left(\frac{-E}{RT}\right).f(\alpha) \quad \textbf{(5)}$$

which can be rearranged and integrated, leading to **Eq. (6)**.

$$g(\alpha) = \int_0^\alpha \frac{d\alpha}{f(\alpha)} = \frac{A}{\beta}.exp\left(\frac{-E}{RT}\right).dT \quad \textbf{(6)}$$

where *g(α)* is the integral form of the reaction model. The conversion dependence of the reaction model, *f(α)*, can be expressed with different mechanisms; some of them are listed in **Table 1**. For a constant heating rate program, the integral in **Eq. (6)** does not have an analytical solution. Consequently, this lays the basis for a number of approximate solutions which gave rise to a variety of approximate integral methods.

Table 1 Algebraic expressions for reaction model *f(α)* for the most frequently used mechanisms

Mechanism	Symbol	*f(α)*
1D diffusion	D1	$½\alpha$
2D diffusion	D2	$1/[-\ln(1-\alpha)]$
3D difussion	D3	$(3(1-\alpha)^{2/3})/\{2[1-(1-\alpha)^{1/3}]\}$
4D diffusion	D4	$3/\{2[(1-\alpha)^{-1/3}-1]\}$
Power law	Pz	$z\alpha^{(1-1/z)}$
Avrami-Erofeev, JMA model	A_p $(0.5 \le p \le 4)$	$p(1-\alpha)[-\ln(1-\alpha)]^{(1-1/p)}$
Sestak-Berggren	$SB_{(n,m)}$	$\alpha^n(1-\alpha)^m$
Sestak-Berggren modified	$SB_{(n,m,z)}$	$\alpha^n(1-\alpha)^m[-\ln(1-\alpha)]^z$

The purpose of the kinetic analysis of a thermally stimulated process is to establish mathematical relationships between the process rate, the conversion, and the temperature. The simplest way is by determining a kinetic triplet: *A*, *E*, *f(α)* or *g(α)*. For a single-step process, assessing the kinetic triplet and substituting it in **Eq. (6)** should be enough to predict the kinetics of the process for any desired temperature program.

2.1. Isoconversional methods

Basic problems of kinetic processing of non-isothermal data determined from thermal analysis measurements can be solved by isoconversional methods. These methods are frequently called 'model-free methods' because of the absence of any assumptions regarding the mechanisms that take place during the degradation of the samples. They give information about the variation of the apparent activation energy (*E*) as a function of the degree of conversion (*α*). The general instructions for the performance of these methods have been given by the International Confederation for Thermal Analysis and Calorimetry (ICTAC) [21,26].

When an isoconversional method is used, the isoconversional principle should be fulfilled. The principle states that the reaction rate at constant extent of reaction is only a function of the temperature. In that way, **Eq. (7)** is obtained by taking the natural logarithmic derivative of the reaction rate (**Eq. (1)**) at α = const.

$$\left[\frac{\partial ln\left(\frac{d\alpha}{dt}\right)}{\partial T^{-1}}\right]_{\alpha} = \left[\frac{\partial ln\,(k(T))}{\partial T^{-1}}\right]_{\alpha} + \left[\frac{\partial ln\,(f(\alpha))}{\partial T^{-1}}\right]_{\alpha} \quad \textbf{(7)}$$

where the subscript α indicates isoconversional values, i.e., the values related to a given extent of conversion. When α = const, $f(\alpha)$ is also constant and, therefore, the second term on the right-hand side of **Eq. (7)** is zero. Accordingly, and taking into account **Eq. (3)**, the following expression is obtained:

$$\left[\frac{\partial ln\left(\frac{d\alpha}{dt}\right)}{\partial T^{-1}}\right]_{\alpha} = -\frac{E_{\alpha}}{R} \quad \textbf{(8)}$$

From **Eq. (8)** the temperature dependence of the isoconversional rate can be used to evaluate isoconversional values of the activation energy, E_{α}, without assuming or determining any particular form of the reaction model. That is why isoconversional methods are commonly called "model-free" methods, as mentioned above. Nevertheless, one should not take this term literally. While the methods do not need to identify the reaction model, they do assume that the conversion dependence of the rate obeys some $f(\alpha)$ model.

The temperature dependence of the isoconversional rate can be obtained experimentally, performing a series of TGA runs with different temperature programs, typically a series of four runs at different heating rates (β). There is a number of integral isoconversional methods that differ in approximations of the temperature integral in **Eq. (6)**. Many of these approximations give rise to linear equations of the general form [26]:

$$ln\left(\frac{\beta_i}{T_{\alpha,i}^{B}}\right) = const - C\left(\frac{E_{\alpha}}{RT_{\alpha,i}}\right) \quad \textbf{(9)}$$

where *B* and *C* are the parameters determined by the type of the temperature integral approximation, and the index *i* indicates the different heating rates. For example, a decent approximation by Murray and White yields *B*=2 and *C*=1 and leads to **Eq. (10)** which is popularly called the Kissinger–Akahira–Sunose (KAS) equation [24].

$$ln\left(\frac{\beta_i}{T_{\alpha,i}^{2}}\right) = const - \frac{E_{\alpha}}{RT_{\alpha,i}} \quad \textbf{(10)}$$

According to **Eq. (10)**, the apparent activation energy E_{α} can be obtained from the slope of the straight line $ln(\frac{\beta_i}{T_{\alpha,i}^{2}})$ vs. $(\frac{1}{T_{\alpha,i}})$ at each given α.

Further increase in the precision can be accomplished by using numerical integration to the results of thermal analysis methods such as thermogravimetry. Vyazovkin [22] developed an advanced integral isoconversional method, in which the effective activation energy value can be determined by minimizing the function expressed by **Eq. (11)**. The temperature integral, **Eq. (12)**, is numerically solved.

$$\Phi(E_{\alpha}) = \sum_{i=1}^{n}\sum_{j\neq 1}^{n}\frac{J[E_{\alpha},T_i(t_{\alpha})]}{J[E_{\alpha},T_j(t_{\alpha})]} \quad \textbf{(11)}$$

$$J[E_\alpha, T(t_\alpha)] = \int_{t_{\alpha-\Delta\alpha}}^{t_\alpha} exp\left[\frac{-E_\alpha}{RT(t)}\right] dt \quad \textbf{(12)}$$

where *i* and *j* denote the different thermal experiments and $\Delta\alpha$ is the conversion increment. Minimization is repeated for each value of α to obtain a dependence of E_α on α.

2.2. Invariant kinetic parameters (IKP) method

The IKP method is based on the "compensation effect" that is observed when a model-fitting method is applied to a single heating rate run. Arranging **Eq. (5)** and replacing it with different algebraic expressions of $f(\alpha)$ (**Table 1**), sets of the Arrhenius parameters ($ln(A_i)$ and E_i) can be obtained after plotting **Eq. (13)** at each heating rate [25].

$$ln\left(\frac{d\alpha}{dT}\frac{\beta_i}{f(\alpha)}\right) = ln\,(A_i) - \frac{E_i}{RT} \quad \textbf{(13)}$$

Although the parameters vary widely with $f(\alpha)$, generally they all demonstrate a strong correlation known as a compensation effect:

$$ln\,(A_i) = a + bE_i \quad \textbf{(14)}$$

The parameters *a* and *b* are the compensation constants that depend on the heating rate. The invariant kinetic parameters, $ln(A_{inv})$ and E_{inv}, are evaluated from several sets of a_j and b_j obtained at different heating rates β_j as **Eq. (15)** shows. This is known as the supercorrelation relation. The IKP are independent of the conversion, the model and the heating rate [25].

$$a_j = ln\,(A_{inv}) - E_{inv}b_j \quad \textbf{(15)}$$

The IKP method can be used only if *E* does not depend on α. This fact should be previously checked by isoconversional methods. Once the invariant parameters are obtained, they can be used to estimate the $f_{inv}(\alpha)$ that best fit the degradation process by introducing the values of E_{inv} and $ln(A_{inv})$ in **Eq. (5)**, giving rise to **Eq. (16)**.

$$f_{inv}(\alpha) = A_{inv}^{-1} exp\left(\frac{E_{inv}}{RT}\right)\beta\frac{d\alpha}{dT} \quad \textbf{(16)}$$

3. Experimental

3.1. Materials

Poly (3-hydroxybutyrate) (PHB, M_w = 492 kg/mol, PDI = 6.3, PHB Industrial S.A., Serrana, SP, Brazil) and poly(lactic acid) (PLA 2003D, M_w = 236 kg/mol, PDI = 3.3, 96 wt% L-isomer, NatureWorks®, Minnetonka, MN, USA) were used as polymeric hosts as received. Tributyrin (TB, 0.302 kg/mol, 98.5% purity), employed as plasticizer, and chitin (Ch, practical grade, powder) from shrimp shells, as well as all chemical solvents, were purchased from Sigma–Aldrich® (Merck KGaA, Darmstadt, Germany).

Chitin nanoparticles (ChNPs) were prepared from purified chitin powder by hydrochloric acid hydrolysis, as presented in our previous work [19]. Size distribution analysis revealed that the average length and diameter of the obtained chitin nanoparticles were 300 ± 170 nm and 40 ± 10 nm, respectively.

3.2. Blends and nanocomposites preparation

Before being processed, PLA, PHB and ChNP were dried overnight at 60 °C in a Cole-Parmer StableTemp vacuum oven (USA) to avoid any moisture trace.

In order to obtain the blends, the raw PLA and PHB pellets were mechanically mixed with the plasticizer (TB) prior to melting in a Haake mixer at 185 °C and a screw rotation speed of 50 rpm for 3 min. The weight ratios of PLA:PHB used were 70:30 and 60:40, while the proportion of TB incorporated was 15 wt% of the final mixture weight, based on previous works [13,14].

Nanocomposites were prepared by incorporating 2 wt% of ChNP into PLA/PHB/TB blends. The processing parameters were a temperature of 185 °C and a screw speed of 60 rpm during a total time of 5 min (3

min for the PLA/PHB blend and 2 min for de nano-component). In this case, the TB was incorporated with the ChNP. The melting process was performed in an inert atmosphere using nitrogen gas to avoid possible oxidation of the ChNP.

Blends and nanocomposites were compression molded at 190 °C in an EMS AMS 160/335DE hydraulic press (Argentina) to obtain the films. The materials were kept between two plates at atmospheric pressure for 1 min until melting and then for 2 min at 5 MPa. Lastly, films were quenched at room temperature.

Neat and plasticized PLA and PHB and polymer blends without TB were also processed in order to be used as reference materials. The samples were designated as listed in **Table 2**.

Table 2 Compositions and names of the obtained materials

Material	Name code	PLA (wt%)	PHB (wt%)	TB (wt%)	ChNP (wt%)
PLA	PLA	100	-	-	-
PLA/TB	PLA/TB	85	-	15	-
PHB	PHB	-	100	-	-
PHB/TB	PHB/TB	-	85	15	
PLA/PHB(7:3)	[a]B73	70	30	-	-
PLA/PHB(7:3)/TB	[a]B73/TB	59.5	25.5	15	-
PLA/PHB(7:3)/TB/ChNP	[a]B73/TB/ChNP	58.1	24.9	15	2
PLA/PHB(6:4)	[a]B64	60	40	-	-
PLA/PHB(6:4)/TB	[a]B64/TB	51	35	15	-
PLA/PHB(6:4)/TB/ChNP	[a]B64/TB/ChNP	49.8	33.2	15	2

[a] The letter B refers to the word -Blend-.

3.3. Thermogravimetric analysis (TGA)

TGA analysis was carried on a Shimadzu TG 50 thermogravimetric analyzer (Japan), the mass of each sample was 8 ± 1 mg and the carrier gas was nitrogen at a flow rate of 50 mL/min. Each sample was heated from room temperature to 500 °C at various heating rate values (5, 15, 30 and 50 °C/min).

3.4. Data processing

The analysis of the kinetic degradation of materials based on PLA/PHB blends was performed taking into account the two-step thermogravimetric behavior, where each step corresponds to the degradation of PHB or PLA, respectively (as later discussed in this article). Thereby, the decomposition processes can be analyzed separately, which allowed the study of each degradation kinetics. Deconvolution of the derivative thermogravimetric analysis (DTG) curves of PLA/PHB blends was performed using a Gaussian multi-peak fit analysis tool in OriginPro 8.5 software (see Supplementary Material for calculation details). The resulting two deconvoluted peaks were designated as D1 for PHB and D2 for PLA. As an example, **Fig. 1** displays the two single curves obtained after the experimental DTG trace of material B73 underwent mathematical deconvolution.

However, a thermogravimetric behavior of three steps was presented by the plasticized polymer blends (PLA/PHB/TB and PLA/PHB/TB/ChNP), with the one corresponding to the plasticizer (D0) being the least stable. In these cases, the three peaks in the DTG curves were deconvoluted, but only the degradation kinetics of the D1 and D2 peaks were studied. The kinetic of the TB degradation peak was not analyzed separately, as it fell outside the scope of this work. It was estimated that it did not significantly affect the degradation of the other components, as TB degradation occurs several degrees before the PHB degradation begins. This approach is consistent with that taken by other authors [27].

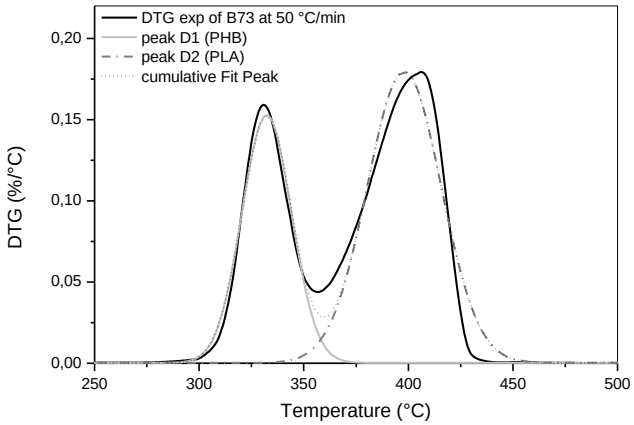

Fig. 1 Deconvoluted peaks and cumulative Fit Peak of B73 DTG curve at 50 °C/min

It should be clarified that studying the degradation kinetics of each peak separately does not imply that the different components present in the different materials do not affect the thermal stability of each other. The variation of the kinetic parameters calculated for each polymer (PHB and PLA) will reflect this. By analyzing D1 and D2 separately, it is possible to individualize and simplify the analysis, trying to approximately explain the actual behavior. Similarly, other research also deals with two decomposition phenomena in a blend separately [28].

4. Results and discussion

4.1. Thermal stability

Thermogravimetric analysis provides valuable information about the thermal degradation behavior of the materials by means of the evolution of the residual mass as a function of temperature (TG) and its first derivative also as a function of temperature (DTG). The initial decomposition temperatures ($T_{2\%}$) were determined from the TG curves as the temperature corresponding to 2% weight loss of the samples, and the maximum weight loss temperatures (T_{max}) were determined from the maximum of DTG curves. The TG and DTG curves of the different produced materials, tested at a heating rate of 15 °C/min, are presented in **Fig. 2**, and collected data are summarized in **Tables 3** and **4**.

Both neat PHB and PLA show one degradation step with maximum degradation temperature (T_{max}) around 305°C and 376°C, respectively, leaving no residue at the end of the test (**Fig. 2a**), indicating that PLA is more thermally stable than PHB. This gap in the thermal degradation temperatures, therefore, is due to the fact that neither their chemical structures are identical nor their degradation mechanisms. PHB thermal degradation occurs by a random chain scission by β-elimination producing mainly crotonic acid and oligomers with crotonate end groups [8,29,30]. Others authors proposed an E1cB mechanism proceeding via intermolecular α-deprotonation by carboxylate anion to produce the same products [31]. Ariffin et al. [32] found that the PHB thermal degradation behavior varied with changes in time and/or temperature. Based on the kinetic analysis of changes in molecular weight, they stated that a non-autocatalytic degradation and an auto-accelerated reaction proceeded in the initial and middle periods, respectively. In contrast, it was reported that PLA decomposes by a non-radical mechanism which involves a back-biting ester interchange reaction to form acetaldehyde, carbon dioxide and monoxide, cyclic oligomer and lactide as products [8,33].

The TG and DTG curves of plasticized polymer samples (PHB/TB and PLA/TB) were also analyzed, and showed a single-step degradation process as well (**Fig. 2a**). In this regard, it was observed that the addition of the plasticizer did not modify significantly the T_{max} of the pure polymers while it caused a marked decrease in the $T_{2\%}$ (around 75.5 °C and 139 °C for PHB and PLA, respectively) due to the degradation of the low molecular-weight plasticizer (TB) (**Table 3**). These results are in agreement with those obtained by other authors for PLA [34,35] and PHB [36] blended with different plasticizers.

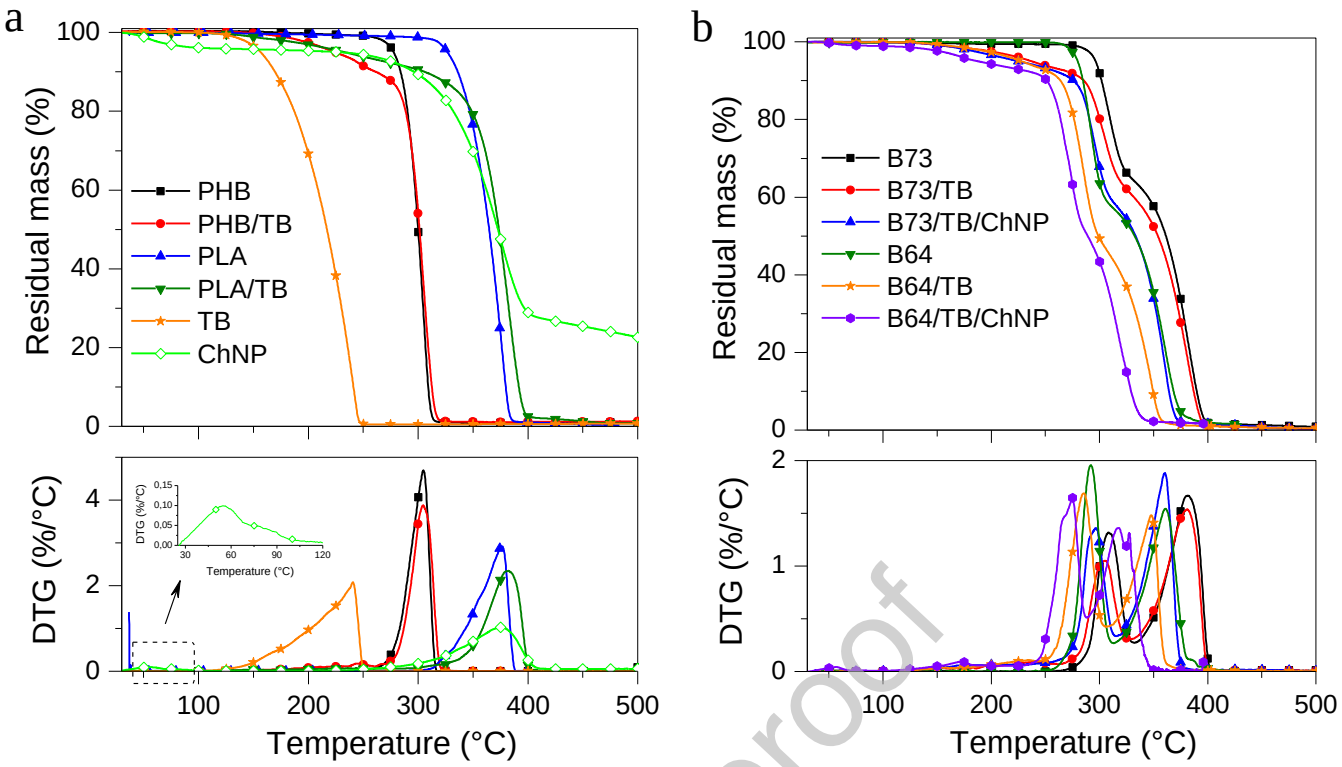

Fig. 2 TG (top) and DTG (bottom) thermograms at 15 °C/min of **(a)** PHB, PHB/TB, PLA, PLA/TB, TB and ChNP, **(b)** B73, B73/TB, B73/TB/ChNP, B64, B64/TB and B64/TB/ChNP

Table 3 Initial decomposition ($T_{2\%}$) and maximum degradation rate (T_{max}) temperatures of PHB, PLA, TB and ChNP, obtained at 15 °C/min

Material	TG	DTG
	$T_{2\%}$ (°C)	T_{max} (°C)
PHB	267.6	304.7
PHB/TB	192.1	304.6
PLA	315.2	375.5
PLA/TB	176.0	382.5
TB	141.1	240.5
ChNP	58.7	375.9

Table 4 Initial decomposition ($T_{2\%}$) and maximum degradation rate (T_{max}) temperatures of PLA/PHB blend samples, obtained at 15 °C/min

Material	TG	DTG	
	$T_{2\%}$ (°C)	T_{max} (°C)	
		D1 (PHB)	D2 (PLA)
B73	287.4	308.8	381.3
B73/TB	190.2	305.0	381.0
B73/TB/ChNP	176.8	296.5	360.1
B64	273.2	292.2	361.2
B64/TB	187.3	285.5	347.8
B64/TB/ChNP	143.8	274.6	321.0

Conversely, a two-steps degradation behavior was observed for all the PLA/PHB blends (**Fig. 2b**) with a first peak at lower temperatures (on average around 295 °C) assigned to the PHB thermal degradation and a second degradation peak at higher temperatures (on average around 360 °C) attributed to the PLA degradation, that is in accordance with the polymer thermal individual behavior which was previously obtained. This thermogravimetric behavior suggests immiscibility or partial miscibility between PHB and PLA, in agreement with the results that other authors have reported [10,12,13,37]. As with the pure polymers, the addition of TB into the B73 and B64 blends generated a decrease in the $T_{2\%}$. Moreover, for B73 and B73/TB samples, the degradation curve shape of each polymer (D1 and D2) do not seem to be influenced by the presence of the other polymer (**Table 4**). The T_{max} on the PHB and PLA curves in these blends were found to be practically the same

as those of the pure polymers (**Table 3**). However, lower maximum degradation temperatures were detected at D1 and D2 peaks for B64 and B64/TB. Such decrease could be attributed to the different morphology of the blends when the PLA:PHB weight ratio was changed, which has been analyzed in a previous work [38]. It was reported a better interfacial adhesion between PLA and PHB phases when PLA:PHB ratio is 70:30, noticing a well dispersed small sphere-shaped PHB domains in the PLA matrix. On the contrary, when PLA:PHB is 60:40, PHB domains appear to be arranged as large ellipsoids within the PLA matrix, suggesting a co-continuous morphology formation and a less strong interfacial adhesion. This could lead to a lower thermal stability for B64 and B64/TB. A similar behavior was observed in Navarro et al. and Bo Zhu et al. works [39,40]. They stated that the morphology optimization of PCL/PLA blends leads to an increase in the contact area between the two phases and that allows the heat to be conducted more evenly throughout the system leading to greater thermal stability.

Additionally, the thermal degradation of ChNPs was studied as seen in **Fig. 2a**. The TG and DTG curves revealed that this polysaccharide is thermally degraded in a single-step. The temperature corresponding to the maximum degradation rate (T_{max}) was found to be at around 376 °C (**Table 3**), which corresponds to the depolymerization/decomposition of polymer chains through deacetylation and cleavage of glycosidic linkages [41]. It was also registered a peak centered at around 55 °C, which corresponds to the evaporation of physically adsorbed water [41,42], and it coincides with the temperature corresponding to the 2% weight loss of the sample ($T_{2\%}$) . At 500 °C it was registered a final weight residue of 22%.

The incorporation of the chitin nanoparticles into the B73/TB and B64/TB blends (**Fig. 2b**) produced a reduction in the T_{max} of both D1 and D2 curves, and a reduction in $T_{2\%}$ as well. Lower thermal stability of nanocomposites may be attributed to a catalyzing effect of the degradation products of ChNPs, which appear in the same temperature range of D1 and D2 and promote the polyesters' hydrolysis. The same behavior was observed for PLA/PHB blends reinforced with cellulose nanofibers [43].

4.2. Kinetic analysis

The thermal degradation kinetics of the materials have been studied by evaluating the kinetic parameters (i.e., *E*, *A*, and *f(α)*), using two isoconversional methods under non-isothermal conditions: KAS and Vyazovkin, previously mentioned.

The TG and DTG of pure PHB and PLA curves, measured at different heating rates, are shown in **Fig. 3**. As it was expected, thermogravimetric curves of both polymers shifted to higher temperatures with increasing the heating rate. Similar behavior was observed for the plasticized polymers (PHB/TB and PLA/TB). This dependence makes possible to determine the apparent activation energy associated with the degradation process. Additionally, it was confirmed that the higher the heating rate, the higher the DTG peaks. This trend is observable when mass loss is derived vs. time [44], but not necessarily when it is derived vs. temperature [28]. As an example, Figure S2 of the Supplementary Material shows different curves of mass loss derived with respect to time (%/sec) plotted against temperature for different studied samples. Consequently, the degradation mechanism's dependence on the heating rate is not expected to be strong, which supports the analysis conducted in this study. Moreover, the plots in Figure S2 reveal that the curves' shape remains almost unchanged with different heating rates.

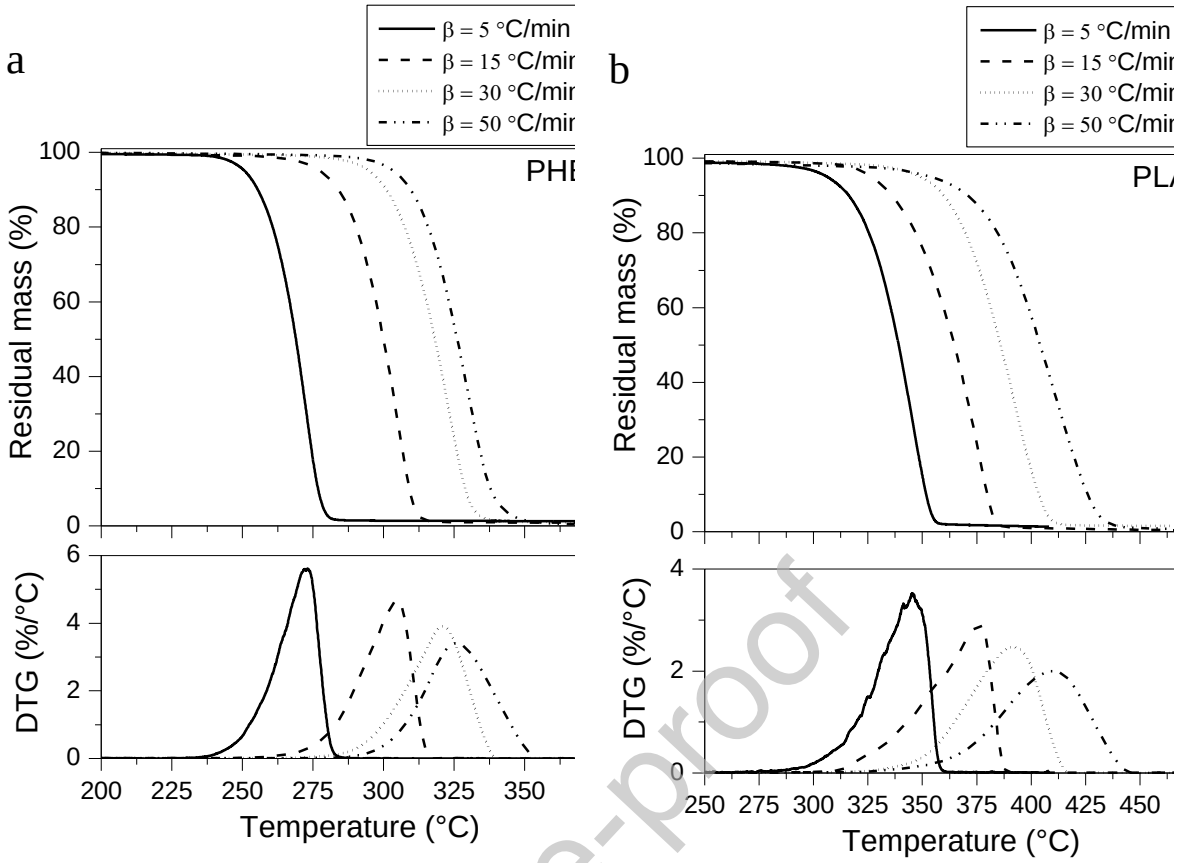

Fig. 3 TG (top) and DTG (bottom) thermograms at various heating rates for **(a)** PHB and **(b)** PLA

The apparent activation energy (E_α) of pure and plasticized PHB and PLA samples was determined using KAS and Vyazovkin methods. **Fig. 4** shows the variation of the E_α and the average temperature (T_{av}) with the degree of conversion (α) for the above-mentioned materials by using both approaches.

The effective activation energy profile, obtained from the experimental degradation data of PHB, remained almost constant with the degree of conversion when KAS (**Fig. 4a**) or Vyazovkin (**Fig. 4b**) methods were employed. Then, it can be assumed the occurrence of a simple one-step process which can be described by a unique kinetic triplet [32,45]. The average E_α calculated for PHB was 95.2 and 86.9 kJ/mol for KAS and Vyazovkin, respectively (**Table 5**). In spite of the fact that the values are quite similar, Vyazovkin method was reported to be more accurate than KAS because it uses numerical integration which is the suitable method to TG data [46,47]. Aoyagi [48] and Kim [49] reported comparable values of E_α for PHB in a narrow range between 111 and 140 kJ/mol. The addition of 15 wt% of TB did not appreciably modify the average value of activation energy for PHB calculated by applying both methods (**Table 5**). However, E_α values at low conversions of PHB/TB sample varied with respect to those of pure PHB, which was related to the lower thermal resistance of the plasticizer compared to that of the pristine polymer, as observed in the TG curve (**Fig. 2a**).

A rather constant value of activation energy was also observed in the whole range of conversion degree of PLA sample (**Fig. 4c** and **Fig. 4d**). The values obtained by applying the two methods are reported in **Table 5**. However, some differences appeared in the dependence of the activation energy with conversion of PLA/TB sample compared to that registered for PLA. Plasticized sample showed lower values of E_α than PLA at low conversions, but it became higher than PLA with the increase of α. That increase in the E_α could be related to the enhancement of chain mobility and intermolecular distance of PLA induced with the TB addition [50].

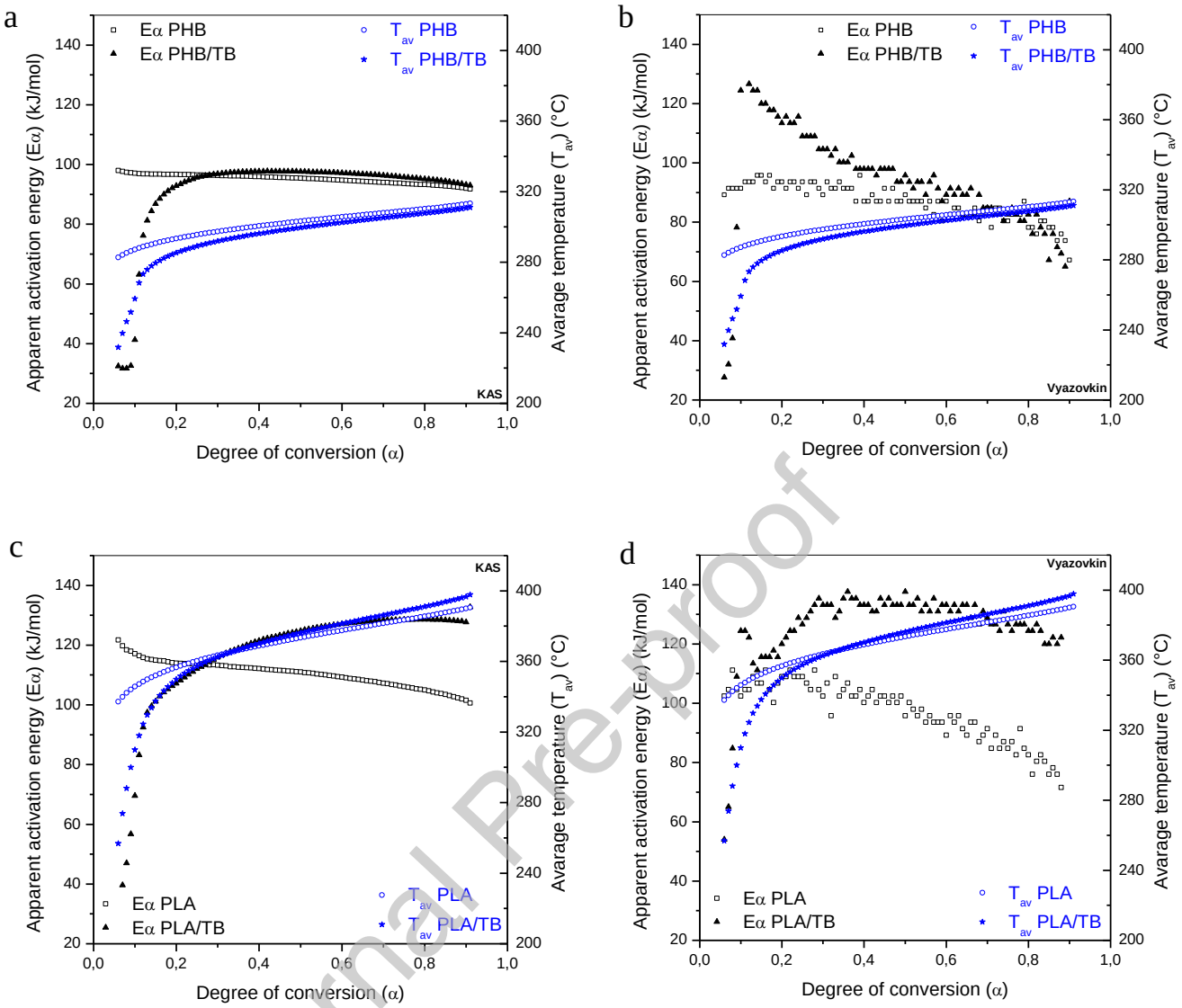

Fig. 4 Apparent activation energy (E_α) and average temperature (T_{av}) vs. degree of conversion (α) for the non-isothermal degradation of: PHB and PHB/TB compositions, applying **(a)** KAS and **(b)** Vyazovkin method; and PLA and PLA/TB compositions, applying **(c)** KAS and **(d)** Vyazovkin method

Table 5 Average values of apparent activation energy (E_α) obtained using the isoconversional methods of Kissinger-Akahira-Sunose (KAS) and Vyazovkin. Values in brackets correspond to the standard uncertainty

Material	KAS				Vyazovkin	
	E_α (kJ/mol)		R^2		E_α (kJ/mol)	
	D1	D2	D1	D2	D1	D2
PHB	95.2 (1.5)		0.985		86.9 (6.0)	
PHB/TB	96.0 (1.7)		0.873		95.0 (13.6)	
PLA		110.4 (4.4)		0.991		95.7 (14.6)
PLA/TB		122.0 (8.0)		0.988		129.6 (11.1)
B73	123.8 (1.5)	173.3 (11.7)	0.912	0.985	117.7 (1.9)	151.5 (8.6)
B73/TB	118.4 (1.9)	158.4 (2.4)	0.966	0.958	117.9 (1.8)	147.6 (1.6)
B73/TB/ChNP	96.4 (0.5)	103.4 (1.9)	0.998	0.991	91.3 (1.6)	99.9 (1.2)
B64	82.7 (0.6)	84.7 (2.8)	0.999	0.990	80.2 (0.8)	75.4 (3.0)
B64/TB	88.8 (2.1)	114.4 (1.8)	0.968	0.989	78.9 (1.5)	109.5 (2.1)
B64/TB/ChNP	56.5 (0.8)	60.4 (0.3)	0.994	0.975	56.7 (0.6)	56.2 (0.4)

As it was observed for the pure polymers, thermogravimetric curves of all the PLA/PHB blends shifted to higher temperatures with increasing the heating rate. **Fig. 5** displays the TG and DTG curves for B73/TB and B64/TB samples at different heating rates, as an example. The remaining curves are shown in the Supplementary Material (Figures S3, S4 and S5). The degradation kinetics of the blends can be studied by analyzing the decomposition processes of PHB and PLA separately. As stated in the Experimental Section, two single curves were obtained after mathematical deconvolution of the experimental DTG data and were used to obtain the profile of the effective activation energy of each component with α throughout the thermal decomposition process.

Fig. 6 shows the variation of the apparent activation energy of PHB and PLA peaks (D1 and D2, respectively) for the B73 and B64 systems, calculated by KAS and Vyazovkin methods. It was observed a similar dependence of E_α with α for D1 and D2 respect to those observed for the pristine polymers, i.e., a rather constant E_α value with α [51]. However, the average values of E_α of each polymer phase differs when they are blended or unblended. The activation energies of the PHB (D1) and PLA (D2) peaks were observed to be higher in the B73 and B73/TB blends compared to those of the unblended pures and plasticized polymers, while they were lower in the B64 and B64/TB blends (**Table 5**). Several factors may contribute to change the thermal degradation behavior of a polymer into a blend [33]. This behavior could be related with the morphology of the blends, as mentioned above, which was also reflected in its mechanical response, as it was observed in our previous works [23,38] where it was stated that the blend B73/TB turned out to be more ductile than the B64/TB. The different interaction between the components and the different morphology may change the energy requirements for thermal degradation.

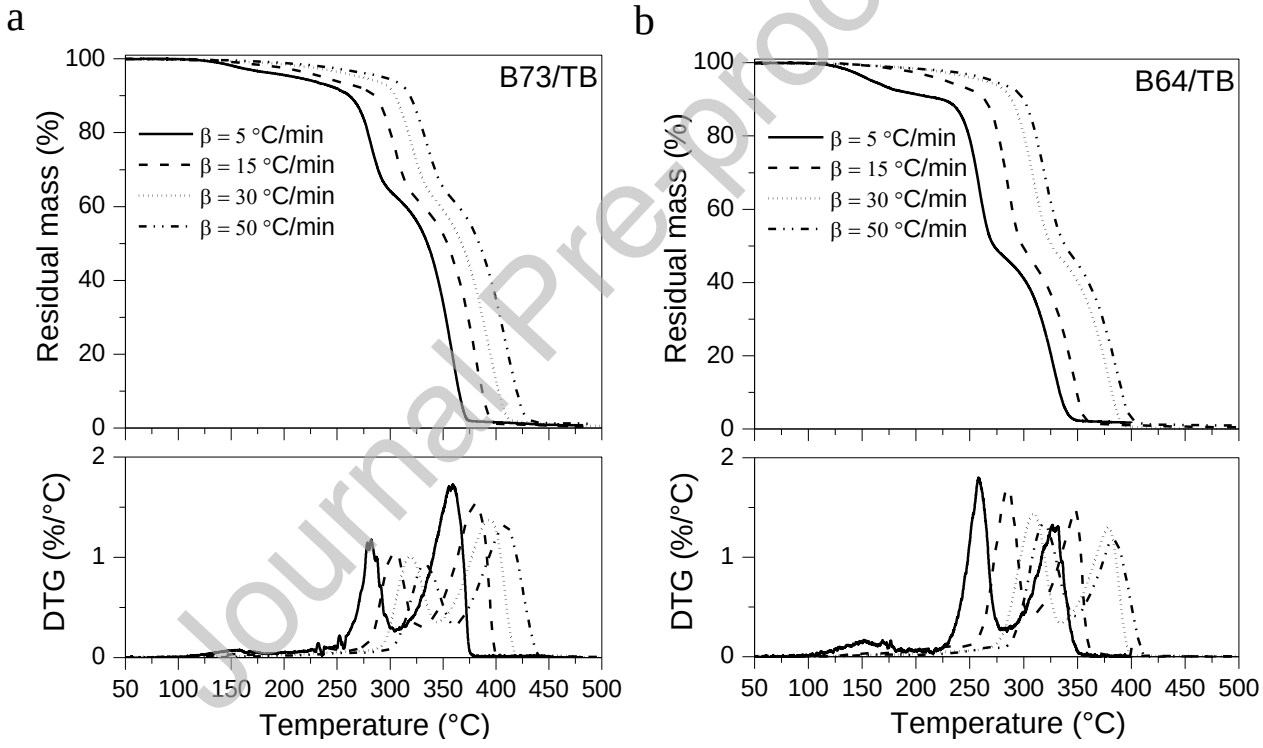

Fig. 5 TG (top) and DTG (bottom) thermograms at various heating rates for **(a)** B73/TB and **(b)** B64/TB

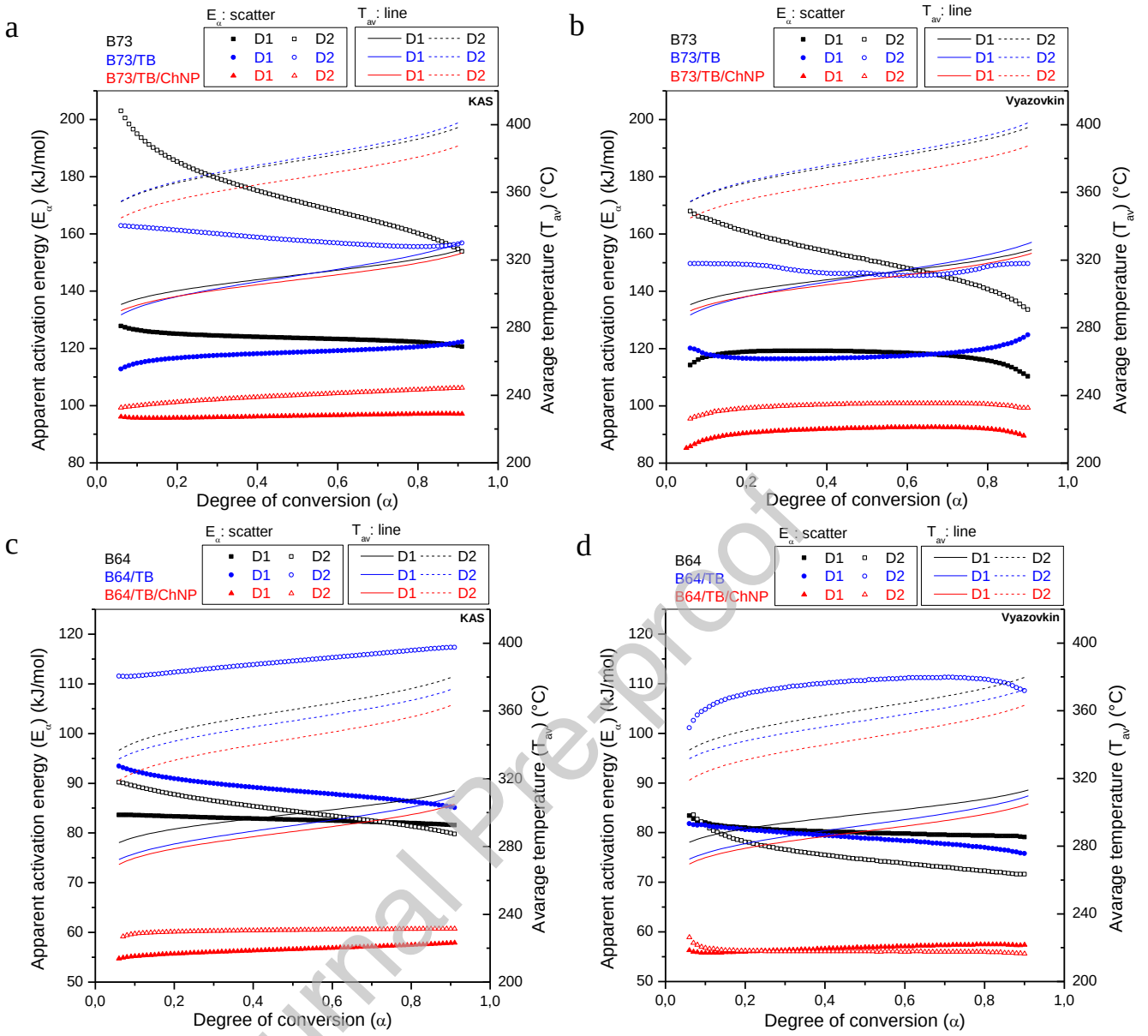

Fig. 6 Apparent activation energy (E_α) and average temperature (T_{av}) vs. degree of conversion (α) for the non-isothermal degradation of: B73 (black), B73/TB (blue) and B73/TB/ChNP (red) compositions, applying **(a)** KAS and **(b)** Vyazovkin method; and B64 (black), B64/TB (blue) and B64/TB/ChNP (red) compositions, applying **(c)** KAS and **(d)** Vyazovkin method. *D1 denotes PHB-deconvoluted peak and D2, PLA-deconvoluted peak*

The effective activation energies were also calculated for the nanocomposites studied and the resulting profiles, obtained from the PHB and PLA deconvoluted peaks (D1 and D2), were plotted as a function of α (**Fig. 6**). The E_α remained practically constant in the whole conversion range for both polymers, which indicates that their thermal degradation proceeds by one step process as well. The average values were also reported in **Table 3**. It was observed a marked diminution in the activation energy values for the nanocomposites obtained for both formulations, in coherence with the thermal stability analysis discussed above, related to the favored hydrolysis of PLA due to a catalysing effect of ChNP. The variation of E_α vs. α for the entire process together with the ones of D1 and D2 for the blend B73 were plotted in Figure S6 (see Supplementary Material), for comparison reasons.

4.3. Estimation of the reaction model

The invariant kinetic parameters (IKP) method was used to predict which kinetic model best describes the thermal degradation process of the blends, which not only involves the effective activation energy, but also the entire kinetic triplet. Once more, the two deconvoluted peaks (D1 and D2) representing the whole

degradation process were used to perform the analysis. As mentioned above, the activation energy remains almost constant in the conversion range comprising D1 and D2, so the IKP method could be applied. Algebraic expressions for the kinetic models of Avrami-Erofeev and Sestak-Berggren shown in **Table 1** were considered. The corresponding *f(α)* models (type A_p, with p =1, 2, 2.5, 3, 4; $SB_{(n,m)}$ with n, m = 0.4, 0.3; 0.4, 0.4; 0.5, 0.5; 0.6, 0.4) were substituted in **Eq. (5)** and fitted to experimental data resulting in different pairs of the Arrhenius parameters, preexponential factor (A_i) and activation energy (E_i). The diffusion models were not considered to enhance the accuracy of the correlation [47]. The compensation effect was verified for all the systems studied, obtaining straight lines for each heating rate by plotting $ln(A_i)$ vs. E_i. **Fig. 7** shows, as an example, the compensation relationship for PLA.

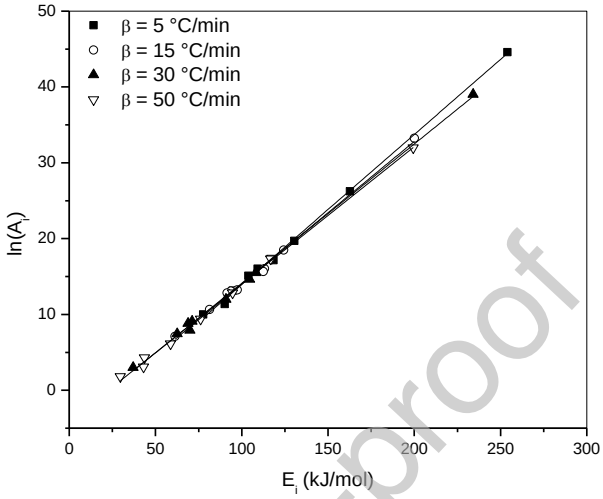

Fig. 7 Compensation effect for the non-isothermal degradation of PLA using models type A_p and $SB_{(n,m)}$

The compensation parameters a_j and b_j at each heating rate were calculated from the intercepts and slopes of these lines, respectively. The resultant a_j and b_j parameters for all systems are plotted in **Fig. 8**, showing a good correlation for all specimens investigated, which means that the existence of a supercorrelation relation is possible.

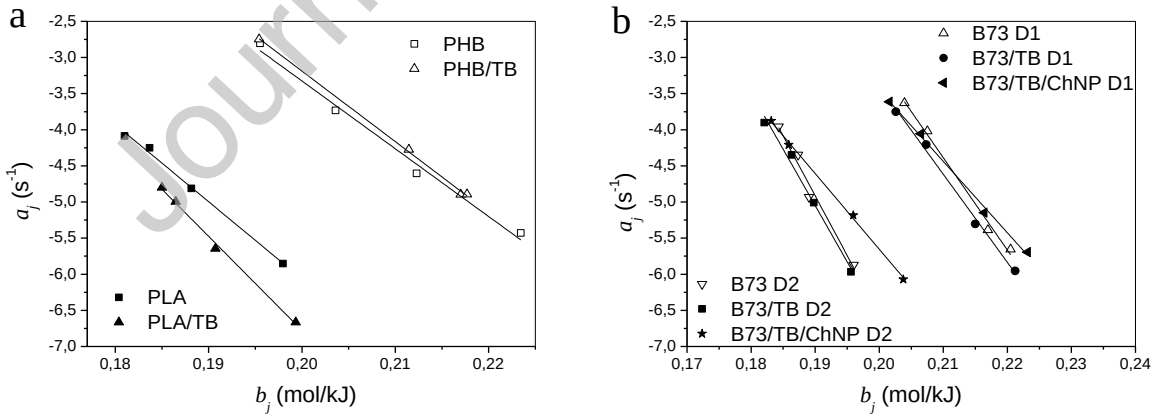

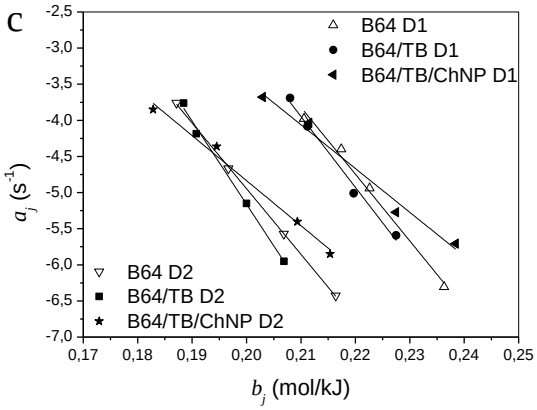

Fig. 8. Supercorrelation relationship for **(a)** pure PLA and PHB, **(b)** B73 blends for D1 and D2, and **(c)** B64 blends for D1 and D2

Then, the invariant kinetic parameters, E_{inv} and A_{inv}, were evaluated using the supercorrelation relation, **Eq. (15)**, and calculated from the slope and the intercept of the lines in **Fig. 8**, respectively. The values of the invariant parameters estimated for both peaks are shown in **Table 6**. All activation energy values are in very good agreement with the estimated values showed in the previous section in **Table 5**.

Table 6 Average values of invariant kinetic parameters for the PHB and PLA based materials (D1 and D2 correspond to PHB and PLA peaks, respectively). Values in brackets correspond to the standard uncertainty

Material	**E_{inv} (kJ/mol)**		**$\ln(A_{inv})$ (s^{-1})**		**R^2**	
	D1	D2	D1	D2	D1	D2
PHB	93.80 (6.77)		15.43 (1.41)		0.984	
PHB/TB	97.68 (2.44)		16.35 (0.51)		0.998	
PLA		106.83 (4.84)		15.30 (0.91)		0.994
PLA/TB		130.28 (5.34)		19.28 (1.02)		0.995
B73	127.82 (7.59)	165.62 (18.40)	22.45 (1.61)	26.55 (3.48)	0.990	0.964
B73/TB	121.95 (6.17)	155.93 (11.70)	20.99 (1.31)	24.58 (2.20)	0.992	0.983
B73/TB/ChNP	98.76 (3.99)	104.68 (2.60)	16.30 (0.85)	15.28 (0.50)	0.995	0.998
B64	92.51 (6.16)	90.90 (0.95)	15.61 (1.37)	13.23 (0.19)	0.987	0.999
B64/TB	98.06 (6.81)	115.08 (5.28)	16.65 (1.48)	17.85 (1.04)	0.986	0.993
B64/TB/ChNP	60.63 (5.52)	62.35 (4.65)	8.66 (1.22)	7.64 (0.93)	0.976	0.983

The Sestak-Berggren (SB) equation (**Table 1**) was evaluated in order to estimate the reaction model which best fit the experimental data. The criterion applied by Pérez-Maqueda et al. [52] was used to validate the applicability of the model. Once the accurate kinetic model is considered for $f(\alpha)$, all experimental data should lie on a single straight line by plotting $\ln[(d\alpha/dT)\beta/f(\alpha)]$ vs. $1/T$ (**Eq. (13)**). It was possible to obtain a straight line by applying the Sestak-Berggren model, considering several n and m values. It was reported [53] that the objective of the SB equation is not to extract an adequate kinetic triplet, but rather to allow a kinetic mechanism to be identified. The parameter estimation from the SB equation can be used to identify the solid-state mechanism which should be used to obtain Arrhenius terms, completing the kinetic triplet.

Finally, to estimate the best n, m of the Sestak-Berggren kinetic models, a nonlinear regression analysis was applied for $f_{inv}(\alpha)$ function (**Eq. 16**), using the experimental data and E_{inv} and A_{inv} from the IKP method. As mentioned above, the values obtained for the n and m exponent parameters will give the information about the solid-state mechanism taking place during a degradation process. It can be compared with the theoretical values of the n and m parameters for different model such as the Avrami-Erofeev (first order: n=0, m=1) and 2D interphase-controlled (n=0, m=0.5) models (**Table 1**). The average value of n and m parameters estimated by applying the Sestak-Berggren model are listed in **Table 7**. It can be seen that the values obtained for the PLA/TB sample ($n\approx0$ and $m\approx0.5$) fit to a 2D interface-controlled model; then the Avrami-Erofeev model was also chosen to be used, following the same methodology mentioned above.

It was observed that the Avrami-Erofeev model resulted in single straight lines after applying the Pérez-Maqueda et al. [52] procedure using several *p* values (**Table 7**), for both peaks (D1 and D2) . The slopes and the intercepts of these lines should provide the values of the activation energies and preexponential factors as the initially assumed, and these values are the so-called 'true' values of *E* and *ln(A)* (**Table 8**). Once, to estimate the best *p* values in the Avrami-Erofeev kinetic model, a nonlinear regression analysis was applied for $f_{inv}(\alpha)$ function (**Eq. (16)**). The fittings performed showed a good correlation thus suggesting that the most probable kinetic mechanism of the materials studied obey the Avrami-Erofeev function. This model consider a solid-state decomposition, which produce a new product and a gas following a nuclei growth mechanism. It could be assumed that the degradation process of the studied materials propagates in two dimensions as the *p* values were found to be up to 2. The variation among the *p* values (Table 7) could be explained considering that the model assumes that there exist some limitations to the nuclei growth such as ingestion and coalescence [54] and that the order of the growth rate depends on the nature of the solid reactants.

Table 7 Average values of *n*, *m* parameters from Sestak-Berggren model: $\alpha^n(1-\alpha)^m$ and *p* parameter from the Avrami-Erofeev kinetic model: $p(1-\alpha)[-\ln(1-\alpha)]^{(1-1/p)}$ for the all compositions

Material	n_{aver}		m_{aver}		p_{aver}	
	D1	D2	D1	D2	D1	D2
PHB	0.281		0.197		2.091	
PHB/TB	0.518		0.240		1.904	
PLA		0.233		0.394		1.833
PLA/TB		0.057		0.475		1.788
B73	0.304	0.214	0.810	0.963	1.307	1.187
B73/TB	0.239	0.238	0.881	0.993	1.232	1.300
B73/TB/ChNP	0.238	0.224	0.608	0.643	1.434	1.399
B64	0.316	0.378	0.625	0.755	1.421	1.325
B64/TB	0.263	0.250	0.778	0.739	1.254	1.313
B64/TB/ChNP	0.225	0.231	0.430	0.451	1.724	1.672

Table 8 'True' values of *E* and *ln(A)* after applying the Avrami-Erofeev model. Values in brackets correspond to the standard uncertainty

Material	E_{true} (kJ mol^{-1})		$\ln(A_{true})$ (s^{-1})		R^2	
	D1	D2	D1	D2	D1	D2
PHB	103.87 (1.15)		17.39 (0.24)		0.975	
PHB/TB	113.37 (3.42)		19.44 (0.72)		0.789	
PLA		109.78 (1.02)		15.75 (0.19)		0.975
PLA/TB		136.23 (0.95)		20.36 (0.18)		0.985
B73	108.08 (1.75)	153.69 (1.30)	16.31 (0.33)	24.06 (0.24)	0.949	0.976
B73/TB	123.41 (1.26)	147.40 (1.77)	21.04 (0.26)	22.63 (0.33)	0.966	0.953
B73/TB/ChNP	100.70 (0.74)	108.98 (0.70)	16.58 (0.15)	15.97 (0.13)	0.982	0.986
B64	86.03 (1.13)	83.33 (1.32)	14.04 (0.24)	11.47 (0.25)	0.944	0.922
B64/TB	93.48 (1.03)	101.83 (0.88)	15.62 (0.22)	17.22 (0.18)	0.973	0.981
B64/TB/ChNP	61.83 (0.43)	63.52 (0.45)	8.86 (0.09)	7.81 (0.09)	0.985	0.985

Additionally, the experimentally obtained differential data (dα/dt vs. α) were compared with the modeled one in order to confirm the selected kinetic model (**Fig. 9**). The dα/dt was simulated using the kinetic triplets previously obtained, which were calculated from the IKP method. **Fig. 9** clearly shows that the experimental differential degradation curves are successfully simulated by means of the above calculated kinetic parameters. In accordance with the weight loss curves, the incorporation of ChNP produces an increase in the degradation rate in the whole range of α for D1 and D2. Other kinetic models such as Power Law and Sestak-Berggren modified were tested (see Figure S7 of Supplementary Material) but it was observed that Avrami-Erofeev kinetic model (Figure 9) is the one that better fit the experimental differential degradation curves. In spite of the

simulated curves do not overlap perfectly the experimental data in some ranges of conversion, the simulations replicate the shape of the experimental data rather adequately, especially at conversions higher than 0.3.

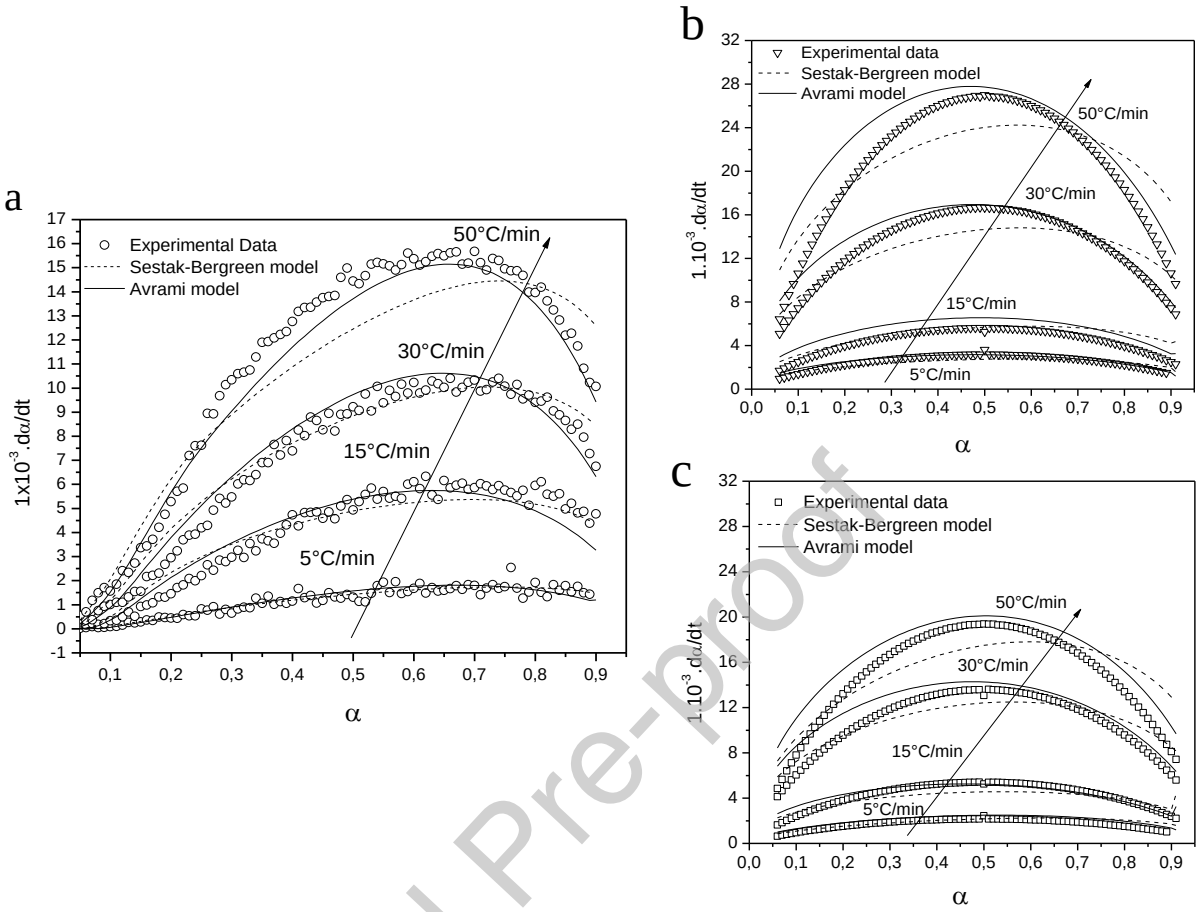

Fig. 9 Comparison of experimental data on the degradation rate vs. conversion with the simulation results obtained using the Sestak-Berggren and Avrami-Erofeev kinetic models at various heating rates for **(a)** PLA/TB and B73/TB/ChNP: **(b)** D1, **(c)** D2

Lastly, the temperature-dependent rate constant (*k)* of the non-isothermal degradation of the materials, expressed using the Arrhenius-type temperature dependence (**Eq. (3)**), can be calculated using the 'true' values of *E* and *ln(A)* (**Table 8**). Curves are presented in **Fig. 10** for the polymers in the blends. Plotting the variation of the *k* with temperature allows us to complete the analysis of the thermal degradation behavior of materials, taking into account both the activation energy and the pre-exponential factor.

At low temperatures, below 200 °C, the rate constants for all samples take very low values, which is consistent with the low degradation rate in this temperature range, as can be seen in the TGA thermograms (**Fig. 2**). As temperature increases, the degradation rate increases exponentially, and for each polymer in every blend this begins to occur in the vicinity of their maximum degradation rate temperature (T_{max}) (**Table 3** and **Table 4**). In this high temperature region, a small increase in reaction temperature will produce a marked increase in the magnitude of the reaction-rate constant. The exponential increase in *k* for PLA in all blends (**Fig. 10b**) starts at higher temperatures than for PHB in all cases (**Fig. 10a**). As activation energy term E_{true} increases, the rate constant *k* decreases and therefore the degradation rate decreases. This can be clearly seen for the flattened curves of PLA in the PLA/TB, B73 (D2) and B73/TB (D2) samples and for PHB in B73/TB (D1) sample for whom the highest activation energies were recorded (**Table 8**). In fact, the highest thermal stability could be assigned to the B73/TB blend since its both polymers, PHB and PLA, presented the lowest rate constant.

The lower thermal stability of B64 blends compared to that of B73 blends, could be detected once again judging by the higher rate constant for both deconvoluted peaks throughout the whole temperature range, according with the previous isoconversional analysis. Furthermore, the addition of ChNP increases the rate constant of blends probably due to the polyesters' hydrolysis boost by the nano- polysaccharide.

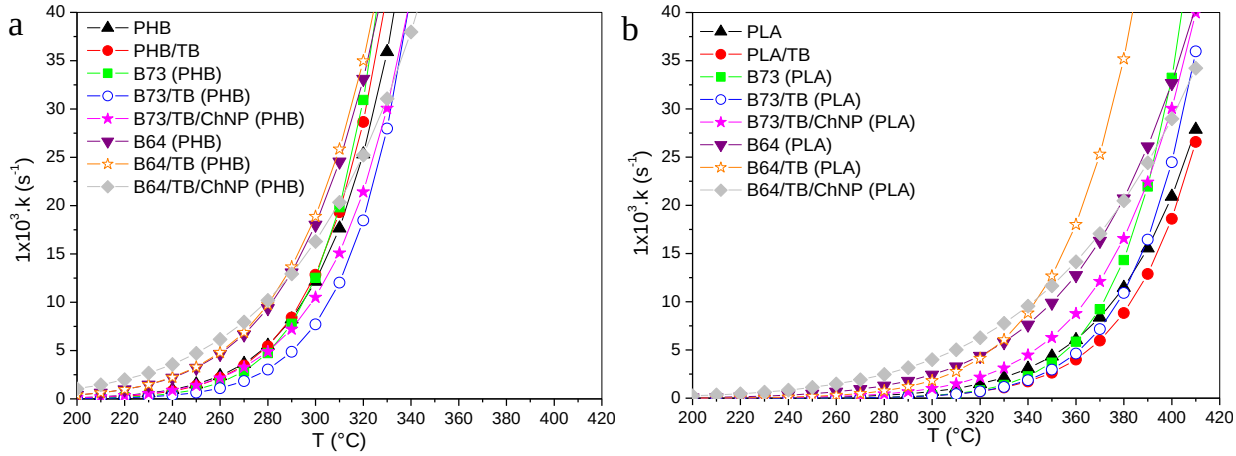

Fig. 10 Dependence of k on T for **(a)** PHB, PHB/TB and deconvoluted D1-peak for all blends, **(b)** PLA, PLA/TB and deconvoluted D2-peak for all blends

5. Conclusions

The thermal degradation kinetics of biodegradable polymer blends based on PLA and PHB was analyzed. It was studied the influence of a plasticizer and chitin nanoparticles on their thermal behavior.

PLA resulted more thermally stable than PHB, showing both of them one degradation step and leaving no residue at the end of the TGA test. The addition of the plasticizer did not modify the T_{max} of the pure polymers while it caused a marked decrease in the $T_{2\%}$ due to the degradation of the low molecular-weight additive.

The TGA results of the blends suggest immiscibility or partial miscibility between PHB and PLA due to the appearance of two peaks attributed to each polymer. Blending the polymers in a ratio 70:30 of PLA:PHB does not seem to influence the thermal stability of each polymer in B73 and B73/TB samples, but lower maximum degradation temperatures were detected for B64 and B64/TB materials, fact that was attributed to the different morphology of blends when the mass ratio is changed. Furthermore, the nanocomposites based on the blends were the samples that showed the lowest thermal stability due to the polyesters' hydrolysis promote by the chitin nanoparticles.

The effective activation energy profile, obtained from the experimental TGA data of PHB and PLA, remained almost constant with the degree of conversion when KAS or Vyazovkin methods were employed. The average values of the activation energies of PHB and PLA peaks were higher in the B73 and B73/TB blends than in the pure and plasticized polymers, while they were lower in the B64 and B64/TB samples, which was related to the different morphology and mechanical behavior of the blends. Finally, the incorporation of chitin nanoparticles into the polymeric matrices produced a remarkable diminution in the activation energy values due to the catalyzing effect of the ChNP.

The invariant kinetic parameters method was applied to the deconvoluted peaks of the blends in order to estimate a pair of kinetic parameters (*A*, *E*). The invariant activation energies calculated were in accordance with the ones estimated by the isoconversional methods. Finally, the Sestak-Berggren equation was used to determine that the most probable kinetic mechanism of the systems studied obeys the Avrami-Erofeev function, which was confirmed by the simulation with the experimental data. Finally, the rate constant of the non-isothermal degradation of the materials, calculated using the Arrhenius-type temperature dependence, was also in accordance with the experimental data.

Acknowledgments The authors gratefully acknowledge the support from the CONICET, ANCyPT (PICT19-2677 and PICT 2021-0153) and the Universidad Nacional de Mar del Plata.

Author Contributions Conceptualization: LBM, VPC, DAD, MLIM. Investigation: MLIM, DAD. Writing—original draft preparation: MLIM, DAD, LBM. Writing—review and editing: MLIM, DAD, LBM, VPC, LM, ITS. All authors have read and agreed to the published version of the manuscript.

Funding This research received no external funding.

Declarations

Conflicts of Interest The authors declare no conflict of interest.

References

[1] V.P. Cyras, N.G. Fernández, A. Vázquez, Biodegradable films from PHB-8HV copolymers and polyalcohols blends: crystallinity, dynamic mechanical analysis and tensile properties, Polym. Int. 48 (1999) 705–712. https://doi.org/10.1002/(SICI)1097-0126(199908)48:8<705::AID-PI205>3.0.CO;2-P.

[2] P. Bordes, E. Pollet, L. Avérous, Nano-biocomposites: Biodegradable polyester/nanoclay systems, Prog. Polym. Sci. 34 (2009) 125–155. https://doi.org/10.1016/j.progpolymsci.2008.10.002.

[3] A.E. Al-Rawajfeh, H.A. Al-Salah, I. Al-Rhael, Miscibility, crystallinity and morphology of polymer blends of polyamide-6/poly(β-hydroxybutyrate), Jordan J. Chem. 1 (2006) 155–170.

[4] V. Siracusa, P. Rocculi, S. Romani, M.D. Rosa, Biodegradable polymers for food packaging: a review, Trends Food Sci. Technol. 19 (2008) 634–643. https://doi.org/10.1016/j.tifs.2008.07.003.

[5] S. Saeidlou, M. a. Huneault, H. Li, C.B. Park, Poly(lactic acid) crystallization, Prog. Polym. Sci. 37 (2012) 1657–1677. https://doi.org/10.1016/j.progpolymsci.2012.07.005.

[6] E. Blümm, A.J. Owen, Miscibility, crystallization and melting of poly(3-hydroxybutyrate)/ poly(l-lactide) blends, Polymer (Guildf). 36 (1995) 4077–4081. https://doi.org/10.1016/0032-3861(95)90987-D.

[7] T. Furukawa, H. Sato, R. Murakami, J. Zhang, Y.X. Duan, I. Noda, S. Ochiai, Y. Ozaki, Structure, dispersibility and crystallinity of poly (hydroxybutyrate)/ poly(l-lactic acid) blends studied by FT-IR microspectroscopy and differential scanning calorimetry, Macromolecules. 38 (2005) 6445–6454. https://doi.org/10.1021/ma0504668.

[8] C. Vogel, H.W. Siesler, Thermal Degradation of Poly(ε-caprolactone), Poly(L-lactic acid) and their Blends with Poly(3-hydroxy-butyrate) Studied by TGA/FT-IR Spectroscopy, Macromol. Symp. 265 (2008) 183–194. https://doi.org/10.1002/masy.200850520.

[9] C. Ni, R. Luo, K. Xu, G.-Q. Chen, Thermal and crystallinity property studies of poly (L-lactic acid) blended with oligomers of 3-hydroxybutyrate or dendrimers of hydroxyalkanoic acids, J. Appl. Polym. Sci. 111 (2009) 1720–1727. https://doi.org/10.1002/app.29182.

[10] M. Zhang, N.L. Thomas, Blending Polylactic Acid with Polyhydroxybutyrate: The Effect on Thermal, Mechanical, and Biodegradation Properties, Adv. Polym. Technol. 30 (2011) 67–79. https://doi.org/10.1002/adv.20235.

[11] L. Chang, E.M. Woo, Crystallization of poly(3-hydroxybutyrate) with stereocomplexed polylactide as biodegradable nucleation agent, Polym. Eng. Sci. 52 (2012) 1413–1419. https://doi.org/10.1002/pen.23081.

[12] Z. Bartczak, A. Galeski, M. Kowalczuk, M. Sobota, R. Malinowski, Tough blends of poly(lactide) and amorphous poly([R,S]-3-hydroxy butyrate) - Morphology and properties, Eur. Polym. J. 49 (2013) 3630–3641. https://doi.org/10.1016/j.eurpolymj.2013.07.033.

[13] D.A. D'Amico, M.L. Iglesias-Montes, L.B. Manfredi, V.P. Cyras, Fully bio-based and biodegradable polylactic acid/poly(3-hydroxybutirate) blends: Use of a common plasticizer as performance improvement strategy, Polym. Test. 49 (2016) 22–28. https://doi.org/10.1016/j.polymertesting.2015.11.004.

[14] M.L. Iglesias-Montes, D.A. D'amico, L.B. Manfredi, V.P. Cyras, Effect of Natural Glyceryl Tributyrate as Plasticizer and Compatibilizer on the Performance of Bio-Based Polylactic Acid/poly(3-hydroxybutyrate) Blends, J. Polym. Environ. 27 (2019) 1429–1438.

https://doi.org/10.1007/s10924-019-01425-y.

[15] M.P. Arrieta, J. López, A. Hernández, E. Rayón, Ternary PLA-PHB-Limonene blends intended for biodegradable food packaging applications, Eur. Polym. J. 50 (2014) 255–270. https://doi.org/10.1016/j.eurpolymj.2013.11.009.

[16] S. Wang, P. Ma, R. Wang, S. Wang, Y. Zhang, Y. Zhang, Mechanical, thermal and degradation properties of poly(d,l-lactide)/poly(hydroxybutyrate-co-hydroxyvalerate)/poly(ethylene glycol) blend, Polym. Degrad. Stab. 93 (2008) 1364–1369. https://doi.org/10.1016/j.polymdegradstab.2008.03.026.

[17] C. Rosales, M.L. Iglesias-Montes, V. Alvarez, Consumer Nanoproducts Based on Polymer Nanocomposites for Food Packaging, in: Handb. Consum. Nanoproducts, Springer Singapore, Singapore, 2021: pp. 1–23. https://doi.org/10.1007/978-981-15-6453-6_103-1.

[18] Q. Guan, H.E. Naguib, Fabrication and Characterization of PLA/PHBV-Chitin Nanocomposites and Their Foams, J. Polym. Environ. 22 (2014) 119–130. https://doi.org/10.1007/s10924-013-0625-8.

[19] M.L. Iglesias-Montes, M. Soccio, V. Siracusa, M. Gazzano, N. Lotti, V.P. Cyras, L.B. Manfredi, Chitin Nanocomposite Based on Plasticized Poly(lactic acid)/Poly(3-hydroxybutyrate) (PLA/PHB) Blends as Fully Biodegradable Packaging Materials, Polymers (Basel). 14 (2022) 3177. https://doi.org/10.3390/polym14153177.

[20] S. Ray, R.P. Cooney, Thermal Degradation of Polymer and Polymer Composites, in: Handb. Environ. Degrad. Mater., Elsevier, 2018: pp. 185–206. https://doi.org/10.1016/B978-0-323-52472-8.00009-5.

[21] M.E. Brown, M. Maciejewski, S. Vyazovkin, R. Nomen, J. Sempere, A. Burnham, J. Opfermann, R. Strey, H.L. Anderson, A. Kemmler, R. Keuleers, J. Janssens, H.O. Desseyn, C.R. Li, T.B. Tang, B. Roduit, J. Malek, T. Mitsuhashi, Computational aspects of kinetic analysis Part A: The ICTAC Kinetics Project-data, methods and results, Thermochim. Acta. 355 (2000) 125–143. https://doi.org/10.1016/S0040-6031(00)00443-3.

[22] S. Vyazovkin, N. Sbirrazzuoli, Isoconversional Kinetic Analysis of Thermally Stimulated Processes in Polymers, Macromol. Rapid Commun. 27 (2006) 1515–1532. https://doi.org/10.1002/marc.200600404.

[23] M.L. Iglesias-Montes, V.P. Cyras, L.B. Manfredi, V. Pettarín, L.A. Fasce, Fracture evaluation of plasticized polylactic acid / poly (3-hydroxybutyrate) blends for commodities replacement in packaging applications, Polym. Test. 84 (2020) 106375. https://doi.org/10.1016/j.polymertesting.2020.106375.

[24] T. Akahira, T.; Sunose, Method of determining activation deterioration constant of electrical insulating materials, Res Rep Chiba Inst Technol (Sci Technol). 16 (1971) 22–31.

[25] A.I. Lesnikovich, S. V. Levchik, A method of finding invariant values of kinetic parameters, J. Therm. Anal. 27 (1983) 89–93. https://doi.org/10.1007/BF01907324.

[26] S. Vyazovkin, A.K. Burnham, J.M. Criado, L. a. Pérez-Maqueda, C. Popescu, N. Sbirrazzuoli, ICTAC Kinetics Committee recommendations for performing kinetic computations on thermal analysis data, Thermochim. Acta. 520 (2011) 1–19. https://doi.org/10.1016/j.tca.2011.03.034.

[27] T. Emiola-Sadiq, L. Zhang, A.K. Dalai, Thermal and Kinetic Studies on Biomass Degradation via Thermogravimetric Analysis: A Combination of Model-Fitting and Model-Free Approach, ACS Omega. 6 (2021) 22233–22247. https://doi.org/10.1021/acsomega.1c02937.

[28] F. Hayoune, S. Chelouche, D. Trache, S. Zitouni, Y. Grohens, Thermal decomposition kinetics and lifetime prediction of a PP/PLA blend supplemented with iron stearate during artificial aging, Thermochim. Acta. 690 (2020). https://doi.org/10.1016/J.TCA.2020.178700.

[29] H. Morikawa, R.H. Marchessault, Pyrolysis of bacterial polyalkanoates, Can. J. Chem. 59 (1981) 2306–2313. https://doi.org/10.1139/v81-334.

[30] A. Ballistreri, D. Garozzo, M. Giuffrida, G. Impallomeni, G. Montaudo, Analytical degradation: An approach to the structural analysis of microbial polyesters by different methods, J. Anal. Appl. Pyrolysis. 16 (1989) 239–253. https://doi.org/10.1016/0165-2370(89)80028-2.

[31] M. Kawalec, G. Adamus, P. Kurcok, M. Kowalczuk, I. Foltran, M.L. Focarete, M. Scandola, Carboxylate-Induced Degradation of Poly(3-hydroxybutyrate)s, Biomacromolecules. 8 (2007) 1053–1058. https://doi.org/10.1021/bm061155n.

[32] H. Ariffin, H. Nishida, Y. Shirai, M.A. Hassan, Determination of multiple thermal degradation mechanisms of poly(3-hydroxybutyrate), Polym. Degrad. Stab. 93 (2008) 1433–1439. https://doi.org/10.1016/j.polymdegradstab.2008.05.020.

[33] J.P. Mofokeng, A.S. Luyt, Morphology and thermal degradation studies of melt-mixed poly(lactic acid) (PLA)/poly(ε-caprolactone) (PCL) biodegradable polymer blend nanocomposites with TiO2 as filler, Polym. Test. 45 (2015) 93–100. https://doi.org/10.1016/j.polymertesting.2015.05.007.

[34] N. Burgos, V.P. Martino, A. Jiménez, Characterization and ageing study of poly(lactic acid) films plasticized with oligomeric lactic acid, Polym. Degrad. Stab. 98 (2013) 651–658. https://doi.org/10.1016/j.polymdegradstab.2012.11.009.

[35] V.P. Martino, R.A. Ruseckaite, A. Jiménez, Thermal and mechanical characterization of plasticized poly (L-lactide-co-D,L-lactide) films for food packaging, J. Therm. Anal. Calorim. 86 (2006) 707–712. https://doi.org/10.1007/s10973- 006-7897-3.

[36] M. Erceg, T. Kovačić, I. Klarić, Thermal degradation of poly(3-hydroxybutyrate) plasticized with acetyl tributyl citrate, Polym. Degrad. Stab. 90 (2005) 313–318. https://doi.org/10.1016/j.polymdegradstab.2005.04.048.

[37] M.R. Nanda, M. Misra, A.K. Mohanty, The effects of process engineering on the performance of PLA and PHBV blends, Macromol. Mater. Eng. 296 (2011) 719–728. https://doi.org/10.1002/mame.201000417.

[38] M.L. Iglesias-Montes, M. Soccio, F. Luzi, D. Puglia, M. Gazzano, N. Lotti, L.B. Manfredi, V.P. Cyras, Evaluation of the Factors Affecting the Disintegration under a Composting Process of Poly(lactic acid)/Poly(3-hydroxybutyrate) (PLA/PHB) Blends, Polymers (Basel). 13 (2021) 3171. https://doi.org/10.3390/polym13183171.

[39] I. Navarro-Baena, V. Sessini, F. Dominici, L. Torre, J.M. Kenny, L. Peponi, Design of biodegradable blends based on PLA and PCL: From morphological, thermal and mechanical studies to shape memory behavior, Polym. Degrad. Stab. 132 (2016) 97–108. https://doi.org/10.1016/j.polymdegradstab.2016.03.037.

[40] B. Zhu, T. Bai, P. Wang, Y. Wang, C. Liu, C. Shen, Selective dispersion of carbon nanotubes and nanoclay in biodegradable poly(ε-caprolactone)/poly(lactic acid) blends with improved toughness, strength and thermal stability, Int. J. Biol. Macromol. 153 (2020) 1272–1280. https://doi.org/10.1016/j.ijbiomac.2019.10.262.

[41] H. Moussout, H. Ahlafi, M. Aazza, M. Bourakhouadar, Kinetics and mechanism of the thermal degradation of biopolymers chitin and chitosan using thermogravimetric analysis, Polym. Degrad. Stab. 130 (2016) 1–9. https://doi.org/10.1016/j.polymdegradstab.2016.05.016.

[42] P. Köll, G. Borchers, J.O. Metzger, Thermal degradation of chitin and cellulose, J. Anal. Appl. Pyrolysis. 19 (1991) 119–129. https://doi.org/10.1016/0165-2370(91)80038-A.

[43] A.N. Frone, D.M. Panaitescu, I. Chiulan, A.R. Gabor, C.A. Nicolae, M. Oprea, M. Ghiurea, D. Gavrilescu, A.C. Puitel, Thermal and mechanical behavior of biodegradable polyester films containing cellulose nanofibers, J. Therm. Anal. Calorim. 138 (2019) 2387–2398. https://doi.org/10.1007/s10973-019-08218-4.

[44] J. Liu, L. Luo, Y. Hu, F. Wang, X. Zheng, K. Tang, Kinetics and mechanism of thermal

degradation of vegetable-tanned leather fiber, J. Leather Sci. Eng. 1 (2019) 9. https://doi.org/10.1186/s42825-019-0010-z.

[45] M. Erceg, T. Kovacic, S. Perinovic, Kinetic analysis of the non-isothermal degradation of poly(3-hydroxybutyrate) nanocomposites, Thermochim. Acta. 476 (2008) 44–50. https://doi.org/10.1016/j.tca.2008.07.009.

[46] I. Srikanth, A. Daniel, S. Kumar, N. Padmavathi, V. Singh, P. Ghosal, A. Kumar, G.R. Devi, Nano silica modified carbon–phenolic composites for enhanced ablation resistance, Scr. Mater. 63 (2010) 200–203. https://doi.org/10.1016/J.SCRIPTAMAT.2010.03.052.

[47] L. Asaro, D.A. D'Amico, V.A. Alvarez, E.S. Rodriguez, L.B. Manfredi, Impact of different nanoparticles on the thermal degradation kinetics of phenolic resin nanocomposites, J. Therm. Anal. Calorim. 128 (2017) 1463–1478. https://doi.org/10.1007/s10973-017-6103-0.

[48] Y. Aoyagi, K. Yamashita, Y. Doi, Thermal degradation of poly[(R)-3-hydroxybutyrate], poly[ε-caprolactone], and poly[(S)-lactide], Polym. Degrad. Stab. 76 (2002) 53–59. https://doi.org/10.1016/S0141-3910(01)00265-8.

[49] K.J. Kim, Y. Doi, H. Abe, Effects of residual metal compounds and chain-end structure on thermal degradation of poly(3-hydroxybutyric acid), Polym. Degrad. Stab. 91 (2006) 769–777. https://doi.org/10.1016/J.POLYMDEGRADSTAB.2005.06.004.

[50] J. Chen, X.A. Nie, J.C. Jiang, Y.H. Zhou, Thermal degradation and plasticizing mechanism of poly(vinyl chloride) plasticized with a novel cardanol derived plasticizer, IOP Conf. Ser. Mater. Sci. Eng. 292 (2018) 012008. https://doi.org/10.1088/1757-899X/292/1/012008.

[51] Y. Márquez, L. Franco, J. Puiggalí, Thermal degradation studies of poly(trimethylene carbonate) blends with either polylactide or polycaprolactone, Thermochim. Acta. 550 (2012) 65–75. https://doi.org/10.1016/j.tca.2012.10.001.

[52] L.A. Pérez-Maqueda, J.M. Criado, F.J. Gotor, J. Málek, Advantages of Combined Kinetic Analysis of Experimental Data Obtained under Any Heating Profile, J. Phys. Chem. A. 106 (2002) 2862–2868. https://doi.org/10.1021/jp012246b.

[53] R.L. Gibson, M.J.H. Simmons, E. Hugh Stitt, J. West, S.K. Wilkinson, R.W. Gallen, Kinetic modelling of thermal processes using a modified Sestak-Berggren equation, Chem. Eng. J. 408 (2021) 127318. https://doi.org/10.1016/j.cej.2020.127318.

[54] A. Khawam, D.R. Flanagan, Solid-state kinetic models: Basics and mathematical fundamentals, J. Phys. Chem. B. 110 (2006) 17315–17328. https://doi.org/10.1021/jp062746a.

Author statement

The authors declare the following contributions:

Conceptualization: LBM, VPC, DAD, MLIM.

Investigation: MLIM, DAD.

Writing—original draft preparation: MLIM, DAD, LBM.

Writing—review and editing: MLIM, DAD, LBM, VPC, LM, ITS.

All authors have read and agreed to the published version of the manuscript.

Magdalena L. Iglesias-Montes (MLIM), David A. D'Amico (DAD), Luciana B. Malbos (LM), Irene T. Seoane (ITS), Viviana P. Cyras (VPC), Liliana B. Manfredi (LBM)

Conflict of Interest

The authors declare that this manuscript contains original research work that has not been published previously and it is not under consideration for publication elsewhere.

Declaration of interests

☒The authors declare that they have no known competing financial interests or personal relationships that could have appeared to influence the work reported in this paper.

☐The authors declare the following financial interests/personal relationships which may be considered as potential competing interests: